

# GRBs: when do blackbody spectra look like non-thermal ones?

S.I.Blinnikov, A.V.Kozyreva, and I.E.Panchenko<sup>1</sup>

Institute for Theoretical and Experimental Physics, 117259 Moscow, Russia  
 Sternberg Astronomical Institute, 119899 Moscow, Russia

## ABSTRACT

We argue that a nonthermally looking spectrum of a gamma-ray burst (GRB) can be formed as a superposition of a set of thermal blackbody spectra. This superposition may be done by time integration which is present even in ‘time resolved’ GRB spectroscopy. A nonthermal spectrum can be obtained also by the space integration which should take place unless all the emission comes from a plane front moving exactly towards the observer. We propose a model of the gamma-ray burst spectrum formation based on this idea. This model allows the GRB radiation to be optically thick and to have higher values of baryon load. Thus the latter is limited by the energy considerations only, and not by the condition of a small optical depth.

*Subject headings:* gamma-rays: bursts — gamma-rays: theory — radiation mechanisms: thermal

## 1. Motivation

Gamma-ray bursts (GRBs) still remain an unresolved mystery of modern astrophysics in spite of recent progress in the observations of their X-ray, optical and radio counterparts. Not only the nature of internal engine, but even the mechanism of gamma-ray emission is unclear. Studying the spectra of GRBs is one of the keys that can unlock this great mystery in future.

Observations of the GRB spectra (Band et al. 1993) show that, in general, they are well described by a low-energy power law with the exponent  $\alpha$ , being exponentially cut off at  $E \sim E_0$ , and by a high-energy power law with the exponent  $\beta$ . Though the values of  $(\alpha, \beta, E_0)$  can be different for individual bursts, they usually are in the range of  $(\sim -1.5 \dots 0.5, -3 \dots 2, 100 \dots 200 \text{keV})$ .

Note that in this paper we consider the photon spectrum  $N(E)$  or  $N(\nu)$ , the differential energy flux density  $F_\nu = h\nu N(h\nu)$ , and  $\nu F_\nu$  distribution. By default, all the power indices in this paper refer to  $N(E)$ .

---

<sup>1</sup>E-mail: blinn@sai.msu.su, sasha@sai.msu.su, ivan@sai.msu.su

The power-law appearance of the spectra can possibly be explained by the hypothesis of their nonthermal origin. The synchrotron shock mechanism (Tavani 1996), where the GRB emission is produced by an optically thin relativistic plasma in a weak magnetic field, is one of those models which give a good agreement with observed spectra. Cohen et al (1997) find that the low-energy spectral index  $\alpha$  in the *time-integrated* of GRB is usually in the range from  $-2/3$  to  $-3/2$  as predicted by the synchrotron shock model. The limits of this range correspond to the synchrotron spectra of instantaneous sample of electrons and the one integrated over their radiative decay (Rybicki & Lightman 1979).

However, Crider, Liang & Preece (1997) have shown, on the basis of the analysis of the *time-resolved* spectra of 99 GRBs, that neither the synchrotron shock nor the simple inverse Compton mechanism can explain the instantaneous GRB spectra and their evolution: the time-resolved spectral slope  $\alpha$  is often outside the limits of the synchrotron model and does not change monotonically with time, as the inverse Compton model predicts.

While these models of gamma-ray bursts (which generally fit the observations) have some difficulties to match them in detail, we can present here a blackbody model that should be at least not worse than the other current ones.

The conflict of the optically thick model for GRBs with observations was discussed already by Paczyński (1986) and Goodman (1986). Paczyński (1986) mentioned: ‘The observed spectra are averaged over large fractions of a second, and this may be responsible for the shallow slope of the low energy part of the spectrum’. The problem was raised recently by Band & Ford (1997). They have posed a question ‘whether burst spectra are narrowband on short time-scales’. So, the question is: are the observed broadband GRB spectra formed by time integrations of an evolving quasi-blackbody instantaneous spectrum, or not. Band & Ford (1997) found no evidence for narrowband emission down to 1 ms time-scale. In the present paper we consider time-scales that are shorter for an observer.

It is well known, that assuming high values of Lorentz factor  $\Gamma$  of the GRB ejecta is necessary to solve the *compactness problem* (Guilbert, Fabian & Rees 1983, Paczyński 1986, Goodman 1986, Krolik & Pier 1991, Rees & Mészáros 1992, Piran 1996). The typical time-scale of the variability of the gamma-ray emission  $\Delta t \sim 10^{-2}$  seconds implies the size of the emitting region  $R < c\Delta t$ , as small as  $\sim 10^3$  km. The enormous number of gamma photons in such a small volume should produce electron-positron pairs which make the emitting region optically thick. This conflicts with the observed nonthermal spectra unless one supposes that the emitting region moves towards the observer at a relativistic speed with Lorentz factor  $\Gamma$ , then its size would be  $\Gamma^2 c\Delta t$ , and the optical depth correspondingly smaller.

We propose an important supplement to this solution of the compactness problem. In our version, the relativistic motion is still required, in order to provide the formation of an integrated spectra from an ensemble of the thermal ones.

It is known that a sum of different thermal blackbody spectra can produce a power-like

spectrum looking as a nonthermal one. It happens, e.g., in the classical case of the Shakura-Sunyaev thin accretion disk (Shakura & Sunyaev 1973). As shown in this paper, a similar approach can provide an analogous result in the case of a relativistically moving emitter.

Evidently, in any realistic situation the spectrum produced by an optically thick body is never a pure blackbody, because of opacity (and hence emission) dependence on wavelength, the effects of sphericity (see Mihalas 1978) etc. For us the black body is just a ‘toy’ model which is however far enough from the spectra of an optically thin plasma, invoked by others for explaining GRBs. Ryde & Svensson (1999) consider another basic model (a non-thermal one) and show that the observed spectra result from the time integration. Our approach is more radical than that.

By the spectrum formation model presented in this paper we do not introduce a new physical model of gamma-ray bursts. We simply point out the fact that the observed non-thermal spectrum can be produced by an optically thick body. The assumptions needed for this seem not to be very unnatural. If such a picture can be worked out as a physical one (not only the ‘toy’ model), then new classes of GRB models become possible, producing ‘dirty’ fireballs, e.g. by the neutrino annihilation (Goodman, Dar, & Nussinov 1987). On the GRB models with a moderately high baryon load see Woosley (1993), Ruffert et al. (1997), Fuller & Shi (1998), Fryer & Woosley (1998), Popham, Woosley, & Fryer (1998).

## 2. The model of spectrum formation

Let us assume that the emitting surface is moving towards the observer with  $\Gamma \sim 10^3$  – it can be an expanding shell, or a blob, or a ‘bullet’, or an ‘internal shock’ (e.g. Piran 1998) – and producing at each instant a pure blackbody spectrum (which has a resemblance to the real spectra of optically thick plasmas).

Due to the well known effect, if the emitter is moving towards the observer with the velocity  $v$  corresponding to  $\Gamma = (1 - v^2/c^2)^{-1/2}$  then the emitter and observer time-scales differ by a factor of  $2\Gamma^2$  (e.g. Rees & Mészáros 1992, Shaviv & Dar 1995, Piran 1998, Dar 1998). Here and below we assume that all clocks are synchronized in the observer’s rest frame, i.e. the effect is purely kinematical (see Fig.1), moreover it is Galilean, not truly relativistic (in the sense that Relativity plays no role in this effect). The Lorentz factor  $\Gamma$  is here simply a measure of the deviation of  $v$  from  $c$ , and nothing else. The difference of the emitter and observer time-scales means that, for example,  $\tau = 10$  ms, the time of integration by an observer, corresponds to  $\tau' \sim 5$  hours of emission time (Fig.1). During this long time the emitting object can expand and cool significantly, so the spectra it produces in the beginning and at the end of the observation interval  $\tau$  can differ drastically. Therefore, the observed spectrum is formed by an integration of some cooling sample of instantaneous spectra.

For simplicity, we assume that the temperature  $T$  and the area  $A$  of the emitting object

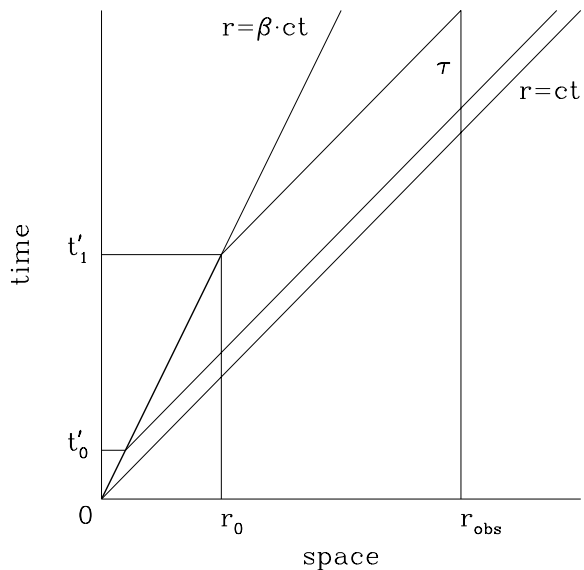


Fig. 1.— The space-time diagram for the emission of a shell expanding with velocity  $\beta c$ . The observer detects the duration  $\tau$  for the pulse emitted by the shell during the interval  $t'_0 \dots t'_1$ .

change with time as described by the following power laws:

$$T = T_0(t/t_0)^{-\theta} = T_0(t'/t'_0)^{-\theta}; \quad A = A_0(t/t_0)^\sigma = A_0(t'/t'_0)^\sigma. \quad (1)$$

Here and below the primed time variables will refer to the emission time, while the non-primed ones - to the detection time.

## 2.1. Analytic treatment

Let us consider a set of arbitrary elementary spectra. If the members of the set have a parameter distributed according to a power law, then the integration of elementary spectra leads quite often to the formation of a power spectrum. Let us show this with a simple example (Fig. 2).

We would like to denote the elementary (instant) spectrum as  $n(E)$ , and the resulting (integral) one as  $N(E)$ . The spectra will be integrated in time from  $t_0$  to  $t_1 = t_0 + \tau$ , where  $t_1 \gg t_0$ .

1. Let the elementary spectrum be  $n(E) \propto E^{-\beta}$  (Fig. 2a) in the high energy part of the spectrum ( $E > E_0$ ) and constant if ( $E < E_0$ ), where  $E_0$  evolves in time like  $t^{-\theta}$  and at  $t_1$  reaches the value  $E_1 = E_0(t_1/t_0)^{-\theta}$ . Then the observed integral spectrum should be

$$N(E) = \int_{t_0}^{t_1} A(t)n(E, t)dt \sim \begin{cases} E^{-\beta}, & E > E_0 \\ E^{-\beta-1/\theta}, & E_1 < E < E_0 \\ \text{const}, & E < E_1 \end{cases}, \quad (2)$$

i.e. have two power-law parts the harder of which reflect the high-energy tail of the elementary spectrum and the softer accounts for the elementary spectrum evolution.

2. Let us now examine the case of a stepwise elementary spectrum (Fig. 2b) described by a Heaviside  $\Theta$ -function:  $n(E) = \Theta(E_0 - E)$ , where  $E_0$  evolves as in the previous example. Then the integral spectrum should be

$$N(E) = \begin{cases} 0, & E > E_0 \\ \sim E^{-\frac{\sigma+1}{\theta}}, & E_1 < E < E_0 \\ \text{const}, & E < E_1 \end{cases}, \quad (3)$$

i.e. the Heaviside step is smoothed into a power function. The discontinuity of the above  $N(E)$  at the point  $E_0$  is an artifact of the approximation: in fact, there is not an exact power function, but very close to it if  $t_1 \gg t_0$  as supposed.

3. So we have shown that the integration of both power and stepwise spectra leads to a power-law behaviour between  $E_1$  and  $E_0$ . The elementary spectrum with Plank (Wien) high-energy tail (Fig. 2c) lies between the power and stepwise cases, it is not as steep as the stepwise one but steeper than the power one. So it is natural to expect a similar result (power-law behaviour) for the integral spectrum.

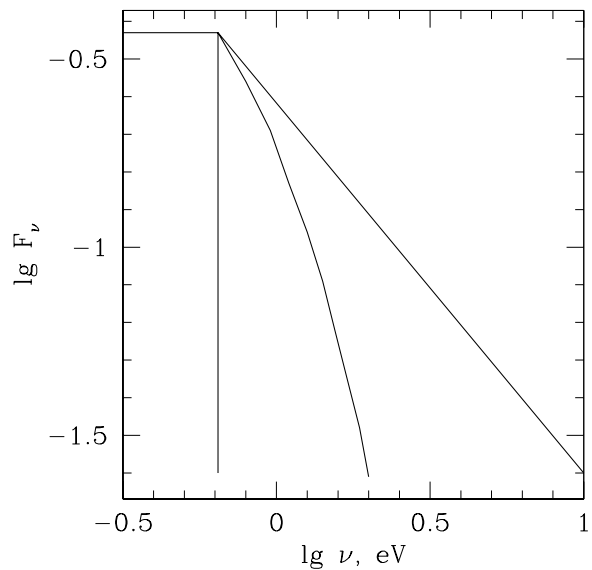


Fig. 2.— The three cases of simple elementary spectra: with the power (a), stepwise (b), and Plank (c) high-energy tails.

## 2.2. The integration of the blackbody elementary spectrum

Now we have come to the time integration of the blackbody Plank spectrum.

$$n(E, t) = A(t) \frac{E^2}{\exp[E/T(t)] - 1}. \quad (4)$$

Here we measure  $E$  and  $T$  in the same units, say,  $T_0$ , and let us measure time in units of  $t_0$ , so instead of

$$A(t) = A_0 \left( \frac{t}{t_0} \right)^\sigma, \quad T(t) = T_0 \left( \frac{t}{t_0} \right)^{-\theta} \quad (5)$$

we have simply

$$A(t) = A_0 t^\sigma, \quad T(t) = t^{-\theta}. \quad (6)$$

The observed integral spectrum is

$$N(E) = \int_1^{t_1} dt A(t) \frac{E^2}{\exp[E/T(t)] - 1} = A_0 \int_1^{t_1} dt \frac{t^\sigma E^2}{\exp(E t^\theta) - 1}. \quad (7)$$

Introducing  $y = E t^\theta$ , we rewrite this as

$$N(E) = A_0 \frac{E^{2-(\sigma+1)/\theta}}{\theta} \int_E^{E t_1} dy \frac{y^{(\sigma+1)/\theta-1}}{\exp(y) - 1}. \quad (8)$$

From this general expression we derive the asymptotic cases.

1. The most interesting case is when  $E < 1$ , that is  $E < kT_0$  in standard units, and  $E t_1 \gg 1$ . One should remember that  $t_1$  is always greater than unity, so the latter inequality is true when  $E$  is not too small. Then we find, replacing the lower integration limit by zero, and the upper one by infinity,

$$N(E) \simeq A_0 \frac{E^{2-(\sigma+1)/\theta}}{\theta} \int_0^\infty dy \frac{y^{(\sigma+1)/\theta-1}}{\exp(y) - 1}. \quad (9)$$

The value of the integral is not interesting for us now. Thus, we produce a power-law spectrum with the exponent  $2 - (\sigma + 1)/\theta$ . Say, for  $\sigma = 2$  and  $\theta = 3/4$  we find the spectrum  $N(E) \sim \nu^{-2}$ . For  $\sigma = 2$  and  $\theta = 1$  we find the spectrum  $N(E) \sim E^{-1}$  (flat  $F_\nu \sim \nu^0$ ), etc. See the numerical examples below.

2. When  $E \ll 1$  and  $E t_1 \ll 1$ , we have  $y \ll 1$ , so we are in the Rayleigh-Jeans (RJ) regime,  $\exp(y) - 1 \simeq y$ , and

$$N(E) \simeq A_0 \frac{E^{2-(\sigma+1)/\theta}}{\theta} \int_\nu^{E t_1} dy y^{(\sigma+1)/\theta-2} \propto E. \quad (10)$$

3. For high frequencies,  $E > 1$  and  $Et_1 \gg E > 1$ , the flux reduces to

$$N(E) \simeq A_0 \frac{E^{2-(\sigma+1)/\theta}}{\theta} \int_E^{Et_1} dy y^{(\sigma+1)/\theta-1} e^{-y} \sim A_0 \frac{E^{2-(\sigma+1)/\theta}}{\theta} E^{(\sigma+1)/\theta-1} e^{-E} \propto E^1 e^{-E}. \quad (11)$$

So, here, in the Wien regime, for any  $\sigma$  and  $\theta$  we have in standard units  $N(E) \sim E^1 \exp(-E/kT_0)$  [contrary to  $N_b(E) \sim E^2 \exp(-E/kT_0)$  for the blackbody of temperature  $T_0$ ].

### 2.3. Numerical Examples

Fig. 3 presents the results of numerical integration of the 4 cases of elementary spectra with various model parameters. It also illustrates the correctness of the above analytical estimates. One can compare these spectra with fig. 4 from Chiang & Dermer (1998) where a similar time integration is done, but in a different physical situation.

For a fixed pair of  $\sigma$  and  $\theta$  the spectrum consists of two power laws and one exponential (Wien) high-energy part. Therefore, it is in some sense similar to the Band (1993) function which also has two power law parts, so it can be expected to fit the observations as well.

The moderately high energy part ( $E_1 < E < E_0$ ) has the power law spectrum with the the exponent depending both on the cooling ( $\theta$ ) and expansion ( $\sigma$ ) laws. The dynamical range, i.e. the spectral width of this part is  $E_1/E_0 = (t_1/t_0)^{-\theta} \gg 1$ . Of course it depends on the integration time  $\tau = t_1 - t_0 \approx t_1$ , and should be smaller for high temporal resolution. This can be a serious test of the present model.

The highest energy part ( $E > E_0$ ) represents the exponential breakdown, which may be observed or not, depending on the value of  $E_0$ . Also, for such energies, there may exists some other (optically thin?) radiation mechanisms which can provide more intense emission than the proposed blackbody one.

The low energy ( $E < E_1$ ) part of the spectrum in our model should have only one possible value of the slope. This is clear from the analytical considerations:  $\alpha = 1$  (see eqn. 10). This  $\alpha$  is close to be consistent with many observations (Crider et al. 1997), but the observed variety of spectra is much richer, than the simple RJ case, and there are claims that some GRB's do show here the spectra predicted by synchrotron model (Cohen et al. 1997). We can demonstrate, that with a small sophistication our blackbody model can reproduce those spectra as well.

Introducing new parameters is usually a means to improve a fit, but also makes the latter physically less reliable. In what follows, we will keep one parameter constant, let us take  $\sigma = 2$ , as the most natural choice. Instead, we can introduce a physically motivated additional parameter  $f_{\text{hard}}$  as the fraction of the time when the value of  $\theta$  is constant, assuming that after some time,  $f_{\text{hard}}\tau$ , the temperature power law changes. In the examples below, for the fixed  $\sigma$  at constant

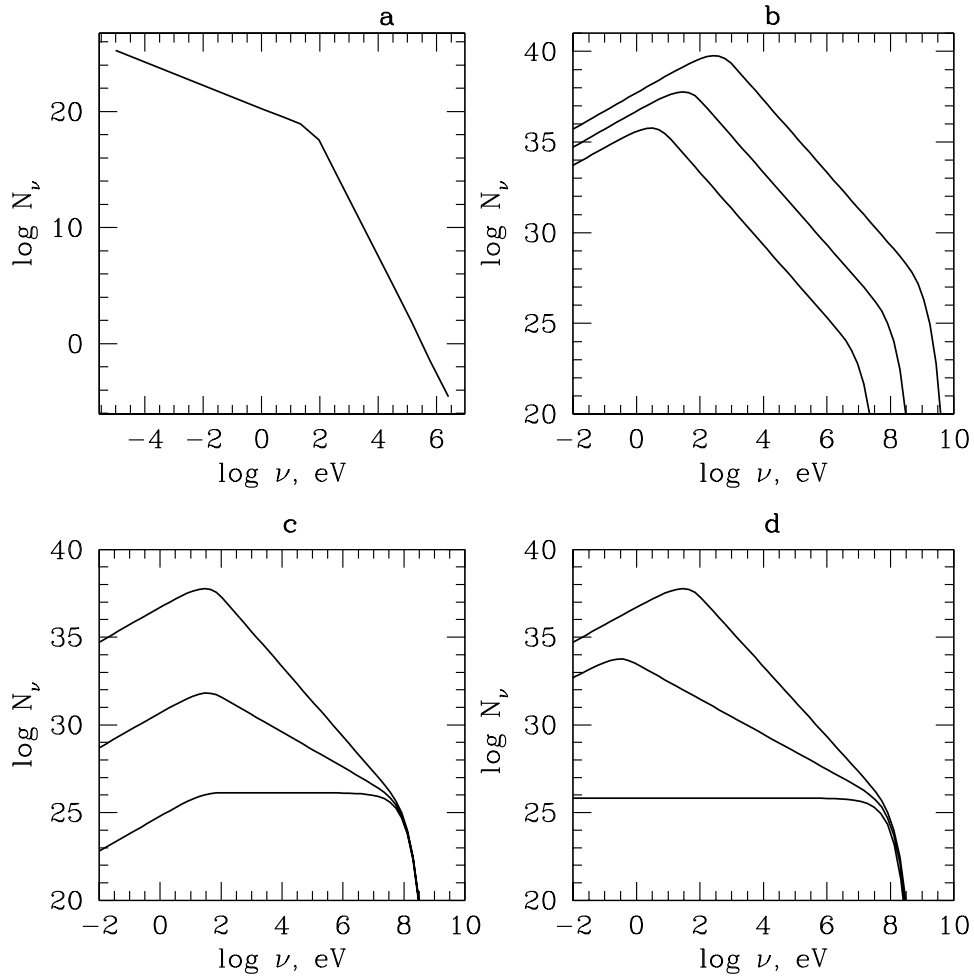


Fig. 3.— The integrated spectra: a) step function with  $T_0 = 10^8 \text{ eV}$ ,  $\sigma = 2$ ,  $\theta = 0.75$ ; b) blackbody with  $T_0 = 10^7, 10^8, 10^9 \text{ eV}$ ,  $\sigma = 2$ ,  $\theta = 0.75$ ; c) the same for  $T_0 = 10^8 \text{ eV}$ ,  $\sigma = 2, 1.25, 0.5$ ,  $\theta = 0.75$ ; d) the same for  $T_0 = 10^8 \text{ eV}$ ,  $\sigma = 2$ ,  $\theta = 1.5, 1, 0.75$

value 2, we allow the value of  $\theta$  to change a bit. For illustration, we have taken GRB spectra given in (Cohen et al. 1997) in the form of postscript files and superimposed them onto our fits. The spectra from (Cohen et al. 1997) are all integrated in time, it would be better to have time-resolved spectra. But in any case it is not possible to have time resolution better than 1 ms and for the illustration of our idea the spectra used are quite good. As shown by Figs. 4, 5, 6, 7, our black body model can provide good fits for the GRB spectra which were claimed to give evidence for synchrotron radiation.

### 3. Discussion and Conclusions

We have assumed that at each moment the spectrum of the gamma-ray burst emission is close to the black body one. After the integration in time over the typical temporal resolution of the observations it produces a spectrum which can be similar to the observed ‘non-thermal’ GRB spectrum. In reality, both the instantaneous spectrum and its true time evolution can deviate significantly from our simplified assumption. So in reality one can have a much richer variety of observed spectra. In our work, we wish only to point out a simple fact: that the observed non-thermal spectrum can be produced by an optically thick expanding body under fairly natural assumptions

We have in mind the following picture. The central engine of GRB operates on a space scale like  $10^6$  cm (the size of a neutron star or a stellar mass black hole). It produces shells or bullets of matter moving with the speed which is only one millionth slower than the light speed  $c$ , i.e. we assume  $\Gamma \sim 10^3$ . The high value of  $\Gamma$  is needed in any case for cosmological GRBs in order to solve the compactness problem (see e.g. Piran 1998 for all refs). But the standard picture invokes the high  $\Gamma$  in order to make the fireball transparent only if it is clean (without baryon load): they have the optical depth  $\tau_{\gamma\gamma}$  going down  $\sim \Gamma^{4+\beta}$ , if the  $\beta \sim 2$  is the index of the power spectrum at the hard tail  $N(E) \propto E^{-\beta}$ .

So in standard picture, and in our picture as well, if we see a pulse of GRB lasting 1 ms, the size of the shell should have grown from  $10^6$  cm up to  $10^6$  light milliseconds =  $10^3$  light seconds  $\sim 10^{14}$  cm, since  $R \sim 2\Gamma^2 c \times 1$  ms. Now one can only start speculating, where do the next pulses of GRB come from. These can be internal or external shocks (Piran 1998), or light reflections (Shaviv & Dar 1995, Drozdova & Panchenko 1997), etc. However, there are arguments (Fenimore, Ramirez, & Sumner 1997) that one shell expanding forever is not able to produce GRB pulses which only show a slight ‘hard to soft’ evolution for hundreds of pulses. Already for the first pulse the shell had to expand from  $\sim 10^6$  cm to  $\sim 10^{14}$  cm. Therefore, a model where a central engine repeats shooting shells or bullets for the whole duration of the GRB is preferred (see also Dar 1998).

Thus, we have  $R$  like  $10^6$  cm and  $t_0 \sim 3 \cdot 10^{-5}$  sec, and  $t_1$  (or  $\tau$ ) like  $10^3$  second, so 7 orders of magnitude for the dynamical range of a power-law spectrum in our model is quite plausible. This

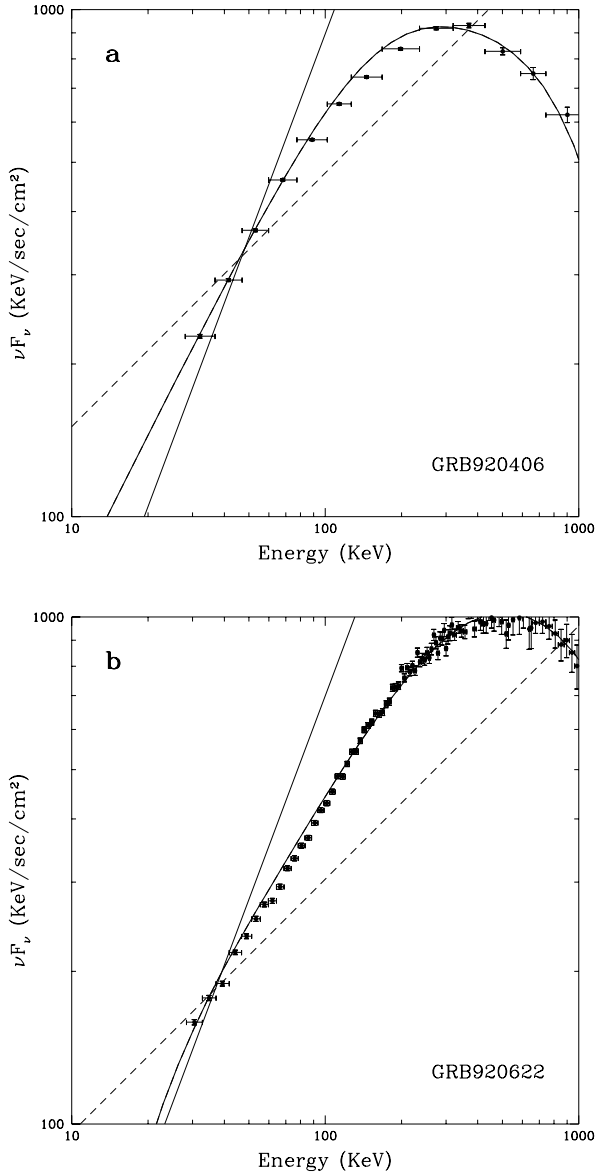


Fig. 4.— a) GRB920406:  $\theta = 0.75$ ,  $\theta_s = 1.0$ ,  $\lg T_0 = 5.45$ ,  $t_1/t_0 = 1.2 \cdot 10^3$ ,  $f_{\text{hard}} = 0.0115$ ; b) GRB920622:  $\theta = 0.75$ ,  $\theta_s = 0.955$ ,  $\lg T_0 = 5.62$ ,  $t_1/t_0 = 1.7 \cdot 10^2$ ,  $f_{\text{hard}} = 0.05$

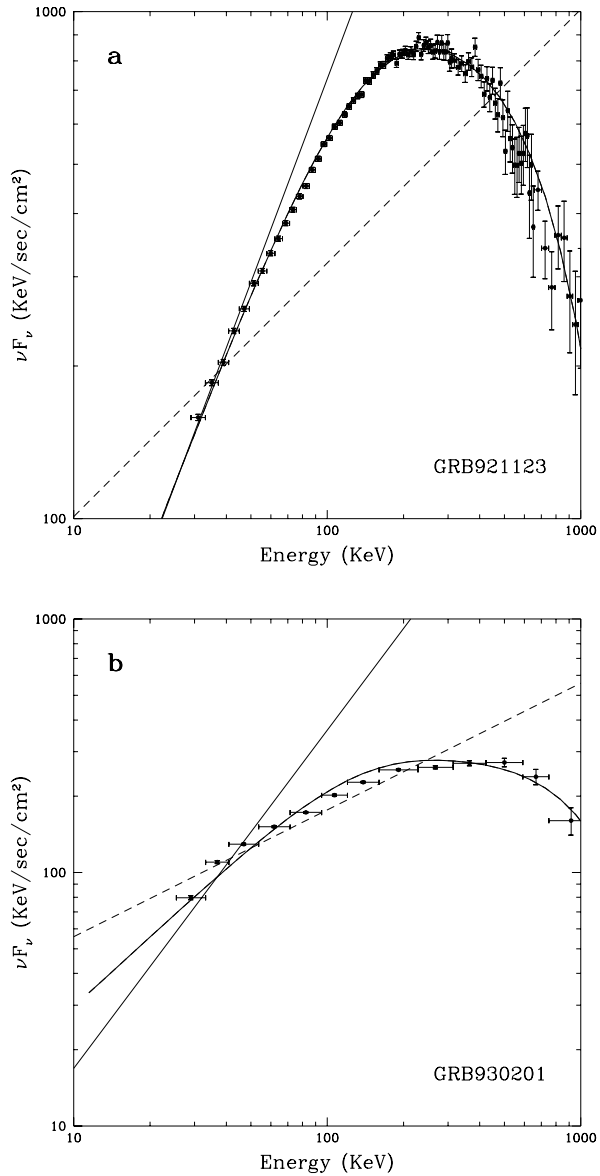


Fig. 5.— a) GRB921123:  $\theta = 0.75$ ,  $\theta_s = 1.125$ ,  $\lg T_0 = 5.28$ ,  $t_1/t_0 = 8.7 \cdot 10^2$ ,  $f_{\text{hard}} = 0.01$  b)  
GRB930201:  $\theta = 0.75$ ,  $\theta_s = 0.975$ ,  $\lg T_0 = 5.47$ ,  $t_1/t_0 = 1.3 \cdot 10^3$ ,  $f_{\text{hard}} = 0.014$

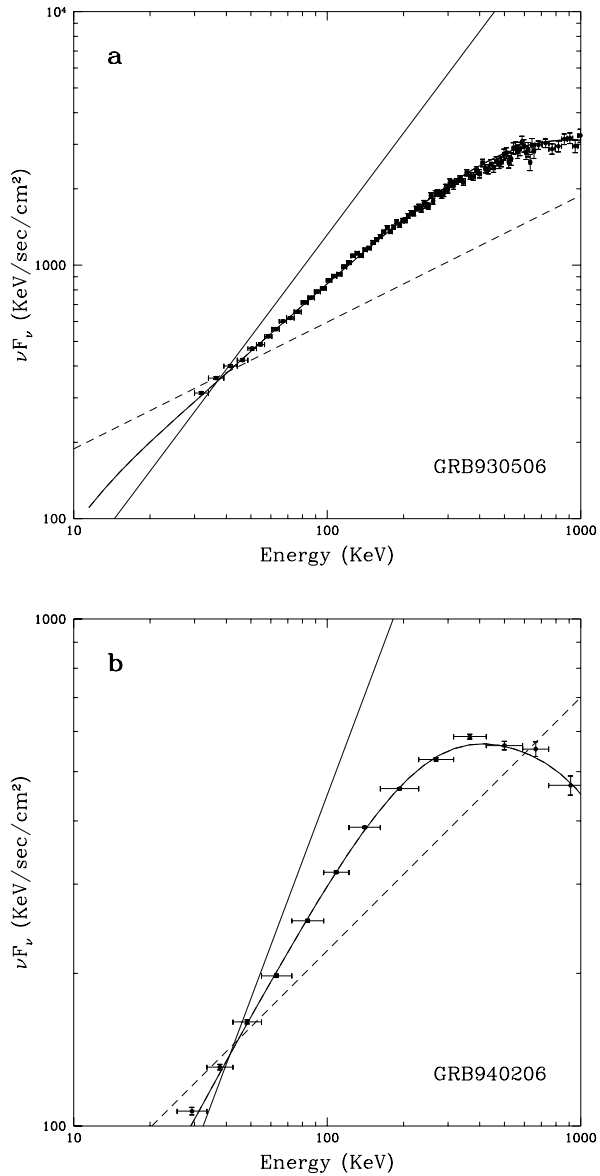


Fig. 6.— a) GRB930506:  $\theta = 0.74$ ,  $\theta_s = 0.967$ ,  $\lg T_0 = 6.0$ ,  $t_1/t_0 = 1.1 \cdot 10^3$ ,  $f_{\text{hard}} = 0.014$  b)  
GRB940206:  $\theta = 0.74$ ,  $\theta_s = 0.975$ ,  $\lg T_0 = 5.65$ ,  $t_1/t_0 = 1.1 \cdot 10^3$ ,  $f_{\text{hard}} = 0.014$

covers the range from keV to GeV. The evidence for hard, TeV, emission associated with GRBs remains inconclusive (Padilla et al. 1998). Only if the extremely hard TeV photons are detected, as suggested by Totani (1998), then one should invoke a truly non-thermal emission mechanism. We do not say that our shell has the thickness in the end like  $\sim 10^{14}$  cm, it must be geometrically thin, so more dense – it is *optically thick*. But its radius  $R$  is of course  $\sim 10^{14}$  cm, with  $dR \ll R$ . It can be *loaded* with baryons to some extend, not violating the energy limits of course (Krolik & Pier 1991). This is good if one has something like stripping the surface layers of neutron stars (Blinnikov et al. 1984; Eichler et al. 1989; Ruffert et al. 1997). Reaching the size  $\sim 10^{14}$  cm our shell (or bullet) has expanded and cooled enough to become transparent in the end. The shell traveled this distance  $10^3$  seconds according to our clocks, but one should not forget that it kept running almost with speed of light, the light that it had produced. So the difference in time of the beginning of the flash, that we see on Earth, and its end is only 1 millisecond. While our shell is still very near the centre, the engine has shot already the second shell (or bullet, Fig. 8), then the 3rd one, ..., the 100th, etc. If the total GRB duration observed on Earth was a few seconds, *all* the shots of the central engine were done when our first shell was like (few seconds/ $10^3$  seconds) smaller than in the end, so its radius was like  $\sim 10^{11}$  to  $\sim 10^{12}$  cm. At this time it was very optically thick, but one should not forget that it moves so fast, that the light of the 2nd, 3rd, ..., 100th etc. shells can reach the first shell only after the first one is far away,  $\sim 10^{14}$  cm from the centre, and absolutely transparent.

If instead of shells we have bullets, moving at some small angles to us there is no problem of transparency. They can cool down and become small solid bodies (this is perhaps not probable, since they must be heated up by ISM).

In reality, not only time, but also space integration takes place. As shown by Rees (1966), (see also Drozdova & Panchenko 1997, Sari 1998) in the case of an expanding emitting shell an observer simultaneously detects radiation produced in different moments of time (thus, with different temperatures) on the ellipsoidal or egg-like surface. The integration over this surface can give the same effect as the integration over time done in this paper, but we do not perform this here because the result strongly depends on the unknown geometry of the emitting surface.

To conclude, we found that a variety of observed ‘nonthermal’ GRB spectra can be well reproduced by the time-integrated emission of a black-body spectra. The most critical test of our model can be the discovery of the temporal resolution dependence of the power spectrum range (here  $E_1 \dots E_0$ ). However, it can be smoothed by a space integration. The main advantage of the proposed model is that it allows the baryon load to be limited not by the optical thickness, but by energy considerations only (one cannot accelerate too much baryons because of their high rest mass).

**Acknowledgements.** Our work is partly supported by RBRF grants 96-02-16352 and 96-02-19756, INTAS ‘Thermonuclear Supernovae’, ISTC 97-370, and Russian Federal programs ‘Astronomy’ and ‘Science Schools’. The work of IEP was made possible by the INTAS 96-0315

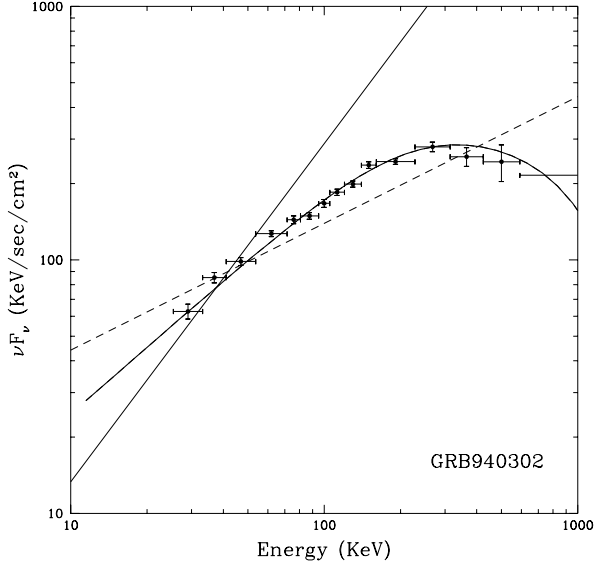


Fig. 7.— GRB940302:  $\theta = 0.75$ ,  $\theta_s = 0.96$ ,  $\lg T_0 = 5.45$ ,  $t_1/t_0 = 7.8 \cdot 10^2$ ,  $f_{\text{hard}} = 0.012$

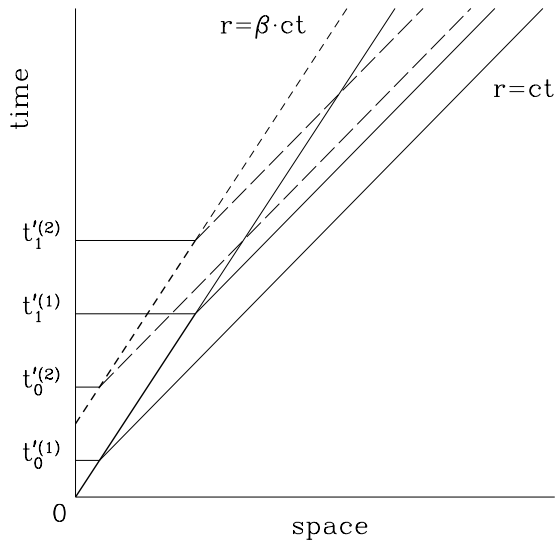


Fig. 8.— The space-time diagram for the emission of two shells. Though the second shell is shot when the first one remains optically thick, the observer sees the radiation of these two shells separately because of their ultra-relativistic velocities.

and RFBR 98-02-16801 grants. Part of the work was done while SIB was visiting Stockholm Observatory under the grant of the Swedish Royal Academy of Sciences, and he is grateful to Peter Lundqvist and Claes Fransson for their hospitality, to Felix Ryde for his data on GRBs, and to Claes-Ingvar Björnsson for stimulating comments. The support of MPA, Garching, and encouragement by Wolfgang Hillebrandt are gratefully acknowledged.

## REFERENCES

Band D. et al., 1993, *ApJ*, 413, 281

Band D., Ford L., 1997, to appear in ‘Gamma-Ray Bursts, 4th Huntsville Symposium’, eds. C. Meegan, R. Preece and T. Koshut (astro-ph/9711327)

Blinnikov S.I., Novikov I.D., Perevodchikova T.V., Polnarev A.G., 1984, *PAZh*, 10, 422; *SvA Letters*, 10, 177

Chiang J., Dermer C., 1998, submitted to *ApJ* (astro-ph/9803339)

Crider A., et al, 1997, *ApJ*, 479, L39

Crider A., Liang E.P., Preece R.D., 1997, to appear in ‘Gamma-Ray Bursts, 4th Huntsville Symposium’, eds. C. Meegan, R. Preece and T. Koshut (astro-ph/9711100)

Cohen E., Katz J.I., Piran T., Sari R., Preece R.L., Band D.L., 1997, *ApJ*, 488, 330 (astro-ph/9703120)

Dar A. 1998, *ApJ*, 500, L93

Drozdova D.N., Panchenko I.E., 1997, *A&A*, 324, 17

Eichler D., Livio M., Piran T., Schramm D. N., 1989, *Nature*, 340, 126

Fenimore E.E., Ramirez E., Sumner M.C., 1997, to appear in ‘Gamma-Ray Bursts, 4th Huntsville Symposium’, eds. C. Meegan, R. Preece and T. Koshut (astro-ph/9712303)

Fryer C. L., Woosley S. E., 1998, *ApJ*, 502, L9

Fuller G. M., Shi X., 1998, *ApJ*, 502, L5

Goodman J., 1986, *ApJ*, 308, L47

Goodman J., Dar A., Nussinov S., 1987, *ApJ*, 314, L7

Guilbert P.W., Fabian A.C., Rees M.J., 1983, *MNRAS*, 205, 593

Krolik J.H., Pier E.A., 1991, *ApJ*, 373, 277

Mihalas D. 1978, Stellar Atmospheres (San Francisco: Freeman

Paczynski B., 1986, ApJ, 308, L43

Padilla L., Funk B., Krawczynski H., et al. (HEGRA collaboration), 1998, A&A, in press  
(astro-ph/9807342)

Piran T., 1996, in *Unsolved Problems in Astrophysics* Eds. Bahcall J. N., Ostriker J. P., Princeton University Press, p.343

Piran T., 1998, to appear in the proceedings of the Fifth Conference on Underground Physics, TAUP97, (astro-ph/9801001)

Popham R., Woosley S.E., Fryer C., submitted to The Astrophysical Journal (astro-ph/9807028)

Rees M., Nature, 1966, 211, 468

Rees M.J., Mészáros P., 1992, MNRAS, 258, 41P

Ruffert M., Janka H.-T., Takahashi K., Schaefer G. 1997, A&A, 319, 122

Rybicki G.B., Lightman A.P., 1979. Radiative Processes in Astrophysics, New York, Wiley & sons

Ryde F., Svensson R., 1999, ApJ, in press (astro-ph/9808213)

Sari R., 1998, ApJ, 494, L49

Shakura N.I., Sunyaev R.A., 1973, A&A, 24, 337

Shaviv N. J., Dar A., 1995, MNRAS, 277, 287

Tavani M., 1996, ApJ, 466, 768

Totani T., 1998, ApJ, 502, L13

Woosley S.E., 1993, ApJ, 405, 273